



Peptide deformylase inhibitors of *Mycobacterium tuberculosis*: Synthesis, structural investigations, and biological results

Arkadius Pichota^{a,*}, Jeyaraj Duraiswamy^a, Zheng Yin^a, Thomas H. Keller^a, Jenefer Alam^a, Sarah Liung^a, Gladys Lee^a, Mei Ding^a, Gang Wang^a, Wai Ling Chan^a, Mark Schreiber^a, Ida Ma^a, David Beer^a, Xinyi Ngew^a, Kakoli Mukherjee^a, Mahesh Nanjundappa^a, Jeanette W. P. Teo^a, Pamela Thayalan^a, Amelia Yap^a, Thomas Dick^a, Wuyi Meng^b, Mei Xu^b, James Koehn^b, Shi-Hao Pan^b, Kirk Clark^b, Xiaoling Xie^b, Carolyn Shoen^c, Michael Cynamon^c

^a Novartis Institute for Tropical Diseases, 10 Biopolis Road, #05-01 Chromos, Singapore 138670, Singapore

^b Novartis Institutes for Biomedical Research, 250 Massachusetts Avenue, Cambridge, MA 02139, USA

^c Veterans Affairs Medical Center, 800 Irving Avenue, Syracuse, NY 13210, USA

ARTICLE INFO

Article history:

Received 10 June 2008

Revised 24 September 2008

Accepted 1 October 2008

Available online 14 October 2008

Keywords:

Mycobacterium tuberculosis

PDF

Antibacterial

SAR

X-Ray

ABSTRACT

Bacterial peptide deformylase (PDF) belongs to a subfamily of metalloproteases catalyzing the removal of the N-terminal formyl group from newly synthesized proteins. We report the synthesis and biological activity of highly potent inhibitors of *Mycobacterium tuberculosis* (Mtb) PDF enzyme as well as the first X-ray crystal structure of Mtb PDF. Structure–activity relationship and crystallographic data clarified the structural requirements for high enzyme potency and cell based potency. Activities against single and multi-drug-resistant Mtb strains are also reported.

© 2008 Elsevier Ltd. All rights reserved.

Tuberculosis (TB), caused by *Mycobacterium tuberculosis* (Mtb), is the most common infectious disease caused by a single bacterium, and it is estimated that two billion people or one-third of the world's population have been infected by Mtb. More than eight million new cases of active TB disease each year result in two million deaths annually, mostly in developing countries.¹ TB is presently treated with a four-drug combination (isoniazid, rifampin, pyrazinamide, and ethambutol) that imposes a lengthy 6- to 9-month treatment course, often under the direct observation of a healthcare provider.² The long treatment time makes patient compliance a challenge and the emergence of multi-drug-resistant Mtb strains (MDR) has limited the available treatment options.³ The situation has recently become even more dire with reports of so called extensively drug-resistant TB (XDR), where especially in HIV/Mtb co-infections all treatment options are failing.⁴ Novel TB drugs are urgently needed to shorten treatment time and to treat drug-resistant TB in a more effective way.

Peptide deformylase (PDF) is a bacterial metalloenzyme which deformylates the N-formylmethionine of newly synthesized poly-

peptides, a key step in protein maturation.⁵ PDF is essential for bacterial growth⁶ making it an appealing target for the design of novel antibiotics.⁷ Naturally occurring antibiotics like actinonin inhibit the activity of the PDF enzyme, and several synthetic PDF inhibitors based on the actinonin scaffold have progressed to pre-clinical and clinical development.⁸

In a previous study, we have validated Mtb PDF as a drug target and shown that the PDF inhibitor LBK-611 (**1**) and analogs have the potential to serve as a new class of antimycobacterial agents.⁹ We report here the structure–activity relationship of analogs of this

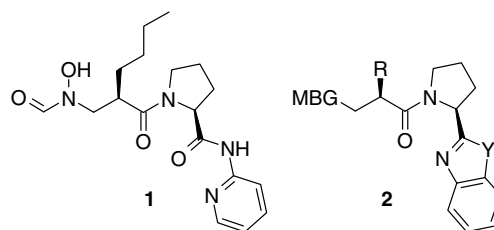


Figure 1. Structures of PDF inhibitor LBK-611 (**1**) and of corresponding bioisosteric PDF inhibitors (**2**).

* Corresponding author.

E-mail address: arkadius.pichota@novartis.com (A. Pichota).

initial lead molecule with the general structure (**2**). The aim of this study was to reduce the peptidic character of the lead compound by introducing benzimidazoles and benzoxazoles ($Y = O, NH$; see Fig. 1) moieties. The synthesis of these amide bioisosters and the corresponding SAR around the metal-binding group (MBG; see Fig. 1) as well as the P1' position (R; see Fig. 1) are reported. Additionally, we describe the first X-ray crystal structure of *Mtb* PDF in complex with inhibitors of general structure **2**.

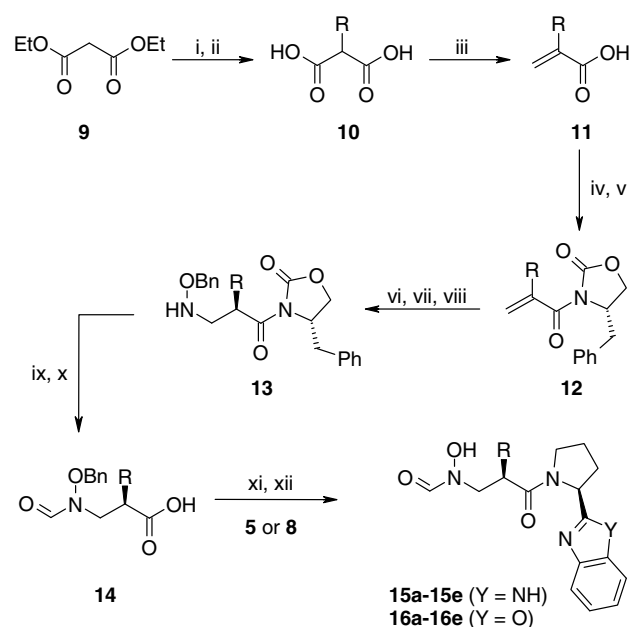
The syntheses of PDF inhibitors used in this study are outlined in Schemes 1–3.¹⁰ (*S*)-2-Pyrrolidin-2-yl-1*H*-benzimidazole (**5**)¹¹ was prepared from *N*-Boc-proline (Boc-**3**) by coupling with 2-amino aniline and followed by imidazole formation in presence of acetic acid¹² at 60 °C as shown in Scheme 1. (*S*)-2-Pyrrolidin-2-yl-benzoxazole (**8**) was prepared from *N*-Cbz-proline (Cbz-**3**) by treatment with ammonia and further conversion of the resulting *N*-Cbz-Pro-NH₂ (**6**) to *N*-Cbz-Pyrrolidine-2-carbonitrile (**7**) with POCl₃ and pyridine.¹³ Treatment of **7** with AcCl in ethanol led to reactive intermediate (*S*)-Pyrrolidine-2-carboximidic acid ethyl ester (not shown in the scheme). Subsequent treatment in situ with 2-hydroxy aniline produced the *N*-Cbz-protected benzoxazole which was followed by hydrogenation to give (*S*)-2-Pyrrolidin-2-yl-benzoxazole (**8**).

The P1' moieties (**14**)¹⁴ containing different R side chains were synthesized as shown in Scheme 2.

Commercially available diethylmalonate (**9**) was alkylated with the corresponding alkyl bromides, and hydrolysis of the ester groups yielded the 2-substituted malonic acids **10**. Subsequent treatment of **10** with formaldehyde in piperidine at 80 °C provided the acrylic acids (**11**). The corresponding mixed anhydrides were obtained by treatment with pivaloyl chloride. Introduction of the chiral auxiliary (*S*)-benzyl-2-oxazolidinone provided **12** and conjugate addition of benzyloxyamine (BnONH₂) formed diastomeric adducts (9:1 ratio of R to S for R = Bu as reported by Pratt et al.¹⁴). The desired (*R*)-diastereoisomer could be isolated as the *p*-toluene sulfonic acid salt. Upon removal of the chiral auxiliary, *N*-formylation provided key P1' fragments **14**. The final compounds, **15a–e** ($Y = NH$) and **16a–e** ($Y = O$), were assembled through standard peptide coupling methodology with **5** or **8**.

Carboxylic acids **19a** and **b** and hydroxamic acids **20a** and **b** were synthesized as shown in Scheme 3. Coupling of (*R*)-2-butylsuccinic acid 4-tert-butyl ester (**18**)¹⁵ with either **5** or **8** provided acids **19a** and **19b**. Subsequent treatment with benzyloxyamine followed by hydrogenation gave the corresponding hydroxamic acids **20a** ($Y = NH$) and **20b** ($Y = O$).

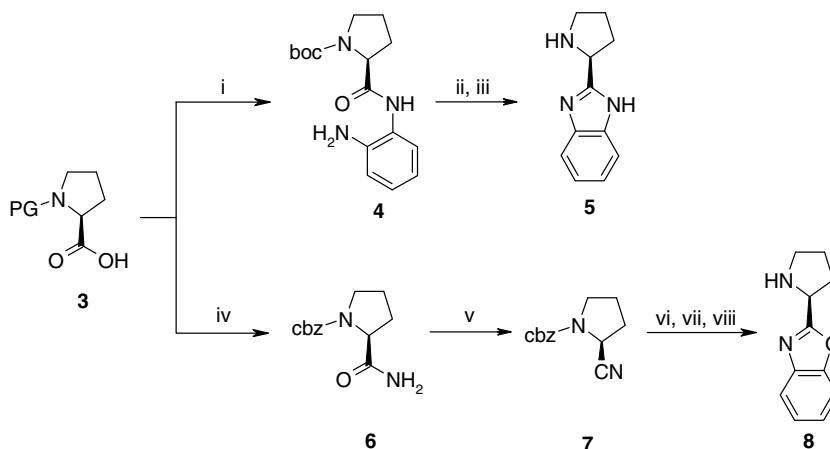
Table 1 summarizes the enzyme inhibition against *Mtb* Ni-PDF enzyme and the whole-cell activity against *Mycobacterium bovis*



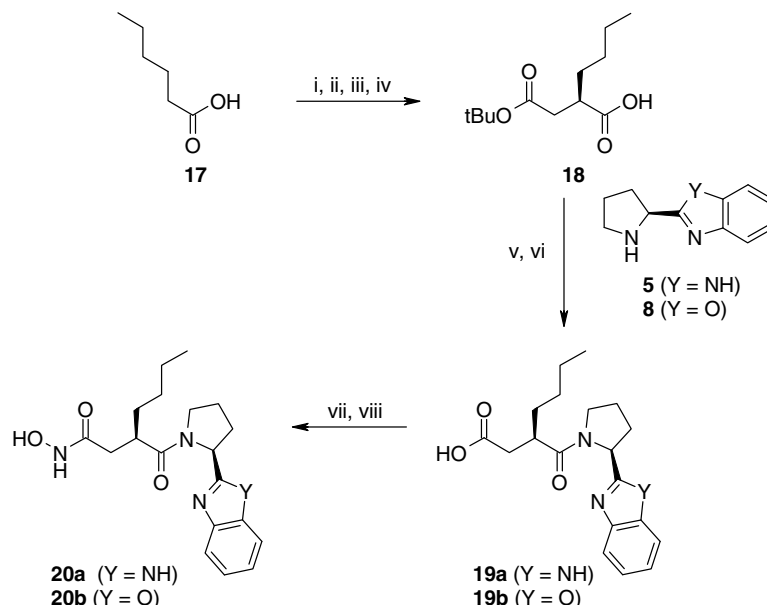
Scheme 2. Reagents and conditions: (i) EtONa, R-Br, EtOH; (ii) KOH; (iii) CH₂O, piperidine, 80 °C; (iv) pivaloyl chloride, NEt(*i*-Pr)₂, THF; (v) (*S*)-4-benzyl-2-oxazolidinone, BuLi, –78 to 25 °C; (vi) BnONH₂ (neat); (vii) *p*-TSA, EtOAc; (viii) Na₂CO₃; (ix) LiOH, 30% H₂O₂, THF–H₂O, 0 °C; (x) HCO₂H, Ac₂O, 0–25 °C; (xi) **5** or **8**, HATU, NEt(*i*-Pr)₂, DMF; (xii) 10% Pd/C, H₂, EtOH.

bacilli Calmette Guerin (*M. bovis* BCG) for compounds with general structure **2**. *M. bovis* BCG was used as surrogate of *Mtb* to evaluate the antibacterial activity of the PDF inhibitors and all biological evaluations were carried out as previously described.⁹

From the data in Table 1, the nature of the chelating group has a marked effect on *Mtb* PDF activity. Carboxylic acids **19a** and **b** are significantly less active than their corresponding hydroxamic acids **20a** and **20b** and reverse hydroxamic acid analogs **15a** and **16a**. The loss in activity can be explained by the relatively poor chelating properties of carboxylic acids with nickel compared to hydroxamic and reverse hydroxamic acids. This trend in activity is also observed in the cell-based screen where the carboxylic acids show no activity against *M. bovis* BCG (>9 µg/ml). The hydroxamic acids, despite their high potency against *Mtb* PDF enzyme, have significantly lower antibacterial activity than the corresponding reverse hydroxamic acid analogs. Additionally, the differences in the



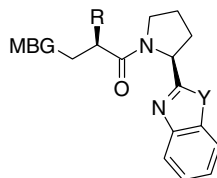
Scheme 1. Reagents and conditions: (i) *N*-Boc-proline (Boc-**3**), 2-Amino aniline, HATU, NEt(*i*-Pr)₂, DMF; (ii) HOAc, 60 °C; (iii) 25% TFA, CH₂Cl₂; (iv) *N*-Cbz-proline (Cbz-**3**), NH₃, MeOH; (v) POCl₃, pyridine; (vi) AcCl, EtOH; (vii) 2-Hydroxy aniline, EtOH, 80 °C; (viii) 10% Pd/C, H₂, EtOH.



Scheme 3. Reagents and conditions: (i) SOCl_2 ; (ii) (S)-4-benzyl-2-oxazolidinone, BuLi, -78 to 25°C ; (iii) NaHMDS, *tert*-butyl bromoacetate, -78 to 25°C ; (iv) LiOH, 30% H_2O_2 , THF– H_2O , 0°C ; (v) **5** or **8**, HATU, $\text{NET}(i\text{-Pr})_2$, DMF; (vi) TFA; (vii) NH_2OBn , EDC, HOBt, DMF; (viii) 10% Pd/C, H_2 , EtOH.

Table 1

PDF–Ni IC_{50} for analogs of **2** and antibacterial activities against *M. bovis* BCG^a



Compound	MBG	R	Y	PDF–Ni IC_{50} (μM)	BCG MIC ($\mu\text{g/ml}$)
15a	N(OH)CHO	Bu	NH	0.010	0.6
15b	N(OH)CHO	Pr	NH	0.024	9
15c	N(OH)CHO	Pentyl	NH	0.015	1.2
15d	N(OH)CHO	Cpm	NH	0.008	1.2
15e	N(OH)CHO	Bn	NH	0.068	>9
16a	N(OH)CHO	Bu	O	0.013	0.6
16b	N(OH)CHO	Pr	O	0.028	4.5
16c	N(OH)CHO	Pentyl	O	0.013	0.6
16d	N(OH)CHO	Cpm	O	0.021	1.2
16e	N(OH)CHO	Bn	O	0.161	>9
19a	COOH	Bu	NH	0.202	>9
19b	COOH	Bu	O	0.803	>9
20a	CONHOH	Bu	NH	0.018	4.5
20b	CONHOH	Bu	O	0.049	4.5

^a For assay conditions see Ref. 9.

benzimidazole and benzoxazoles moieties were found to have little effect on activity in both *Mtb* PDF and *M. bovis* BCG assays.

The observed inhibitory activity of the tested compounds against *Mtb* PDF with respect to different R groups is consistent with the presence of a well defined hydrophobic S1' pocket.¹⁶ The S1' pocket plays a critical role in binding the methionine found in the natural substrate and is as such capable of accommodating small alkyl and cycloalkyl groups. Consequently, inhibitors incorporating hydrophobic R groups like propyl, butyl, pentyl and cyclopentylmethyl displayed potent *Mtb* PDF inhibition. However the incorporation of a benzyl group resulted in a significant loss in enzyme inhibition.

Compounds with similar *Mtb* PDF activity often display different cell-based activity profiles. These differences may be derived

from a combination of bacterial cell wall penetration properties and recognition by an efficient efflux system.¹⁷

The activity against *Mtb* was assessed for LBK-611 (**1**) and two active PDF inhibitors of both series: **15a** and **d** (benzimidazoles) and **16a** and **d** (benzoxazoles) (Table 2).¹⁸ All PDF inhibitors were found to be highly active (0.05–0.2 $\mu\text{g/ml}$) against *Mtb* strain H₃₇Rv¹⁹ and comparable to the gatifloxacin control (average MIC of 0.07 $\mu\text{g/ml}$). As expected for compounds with a new mechanism of action, the PDF inhibitors retain their excellent activity against single and multi-drug-resistant *Mtb* strains (Table 2, **1**, **15a** and **16a**). These results suggest that PDF inhibitors may have potential as antimycobacterial agents against MDR TB.

Structures of several complexes of *Mtb* PDF with our inhibitors were determined at 2.0 to 1.4 Å resolutions. Each of these struc-

Table 2

In vitro antitubercular activity against selected strains of *M. tuberculosis* (MIC in $\mu\text{g/ml}$).

Compound	Mtb H ₃₇ Rv	INH SDR ^a	SM SDR ^b	RIF SDR ^c	PZA SDR ^d	Beijing W MDR ^e
1	0.2 ^f	0.1	0.5	0.25	0.5	0.125
15a	0.1	0.03	0.2	0.125	0.25	0.03
15d	0.05	nd	nd	nd	nd	nd
16a	0.15 ^f	0.06	0.5	0.6	0.25	0.06
16d	0.2	nd	nd	nd	nd	nd

Gatifloxacin was used as positive control (MIC H₃₇Rv = 0.07 $\mu\text{g/ml}$).

^a Isoniazid single-drug-resistant (SDR) strain.

^b Streptomycin-resistant strain.

^c Rifampicin-resistant strain.

^d Pyrazinamide-resistant strain.

^e Beijing W multi-drug-resistant strain.

^f Average value of eight independent experiments.

tures contains a complex of *Mtb* PDF, a bound metal ion (Ni^{2+}) and an inhibitor. The X-ray crystal structure of **16a** with *Mtb* PDF is shown in Figure 2.²⁰

Based on sequence homology, PDFs are typically classified as type I (generally from Gram-negative species) or II (generally from Gram-positive species). Type II PDF has a larger molecular weight than type I PDF, primarily due to sequence insertions; however, the type I PDFs have a longer C-terminal extension than type II. These sequence differences result in structural differences between type I and type II PDFs.¹⁶ Amino acid sequence analysis of *Mtb* PDF indicates that it has some features similar to type I PDF, such as the extended C-terminal portion, while it also has features similar to type II PDF, such as several insertions.²¹ However, the core structure of *Mtb*-PDF is shown to be more similar to that of a typical type I PDF (such as *Escherichia coli* PDF). Similar to *E. coli* PDF, the structure of *Mtb* PDF contains three α -helices, seven β -sheets, and three 3_{10} helices, and all the residues from three highly conserved motifs are structurally conserved forming the active site. The unique feature of *Mtb* PDF is its unusually long C-terminal extension, part of which forms a β -strand pairing with the β -strand from N-terminal region. This extension has been shown to be critical for *Mtb* PDF activity.²² The substrate-binding site of PDF from different bacteria species have been described previously.¹⁶

The X-ray crystal structure of *Mtb* PDF and bound inhibitors were used to identify and explain the structural requirements for the enzyme potency observed. Overall, the structures of *Mtb* PDF-inhibitor complexes reveal that the active-site in *Mtb* PDF is very

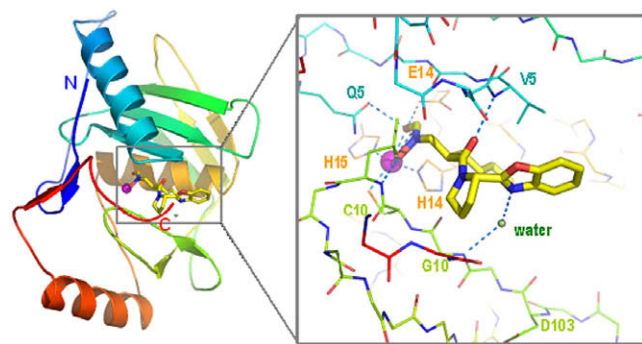


Figure 2. X-Ray crystal structure of **16a** bound to Ni-PDF of *M. tuberculosis*. The Ni^{2+} atom is colored in magenta, nitrogen atoms in blue, and oxygen atoms in red. The compound is shown as yellow stick model in the active site. X-ray analysis revealed that the benzoxazole part is pointing out of the active site pocket. The critical interactions are between the chelating unit and the metal atom, the butyl side chain (methionine mimic), and the central carbonyl atom (H-bond to V5). Atomic coordinates have been deposited in RCSB protein data bank, with accession code 3E3U.

similar to those from other species. The substrate-binding site can be divided into three sub main pockets, termed the S1', S2' and S3' pockets, and the metal-binding site. The S1' pocket is a deep hydrophobic pocket, whereas the S2' and S3' pockets are shallow, less well-defined, solvent exposed surface depressions. The active site of *Mtb* PDF is highly conserved, particularly in the S1' pocket, which is conserved across species. The nickel ion is coordinated by three protein residues (His148, His152 and Cys106) and a bidentate reverse hydroxamic acid moiety, resulting in a square pyramidal coordination. The interactions between *Mtb* PDF enzyme and inhibitor **16a** are illustrated in Figure 2; most of the interactions are with conserved residues, and all H-bond interactions are with protein backbone atoms. The crystal structure of *Mtb* Ni-PDF-**16a** complex (Fig. 2) indicates that substituents at P3' can be well tolerated without affecting PDF activity as their binding site is partially solvent exposed. This finding suggests that this position is ideally suited for the introduction of favorable pharmacokinetic properties through various substituents. This will be described in a separate letter.

In conclusion, we have identified highly potent PDF inhibitors of *Mtb* and established an initial SAR. Several potent inhibitors of *Mtb* PDF were identified which were also highly active against single and multi-drug-resistant strains of *Mtb*, indicating their potential use as antibacterial agents against MDR TB. The X-ray crystal structure of an *Mtb* PDF-inhibitor complex was solved and used to identify the structural requirements for high enzyme potency.

Acknowledgments

The authors thank Jeasie Tan for analytical support, and Kathryn Bracken, Neil Ryder and Beat Weidmann for helpful discussions.

Supplementary data

Supplementary data associated with this article can be found, in the online version, at doi:10.1016/j.bmcl.2008.10.040.

References and notes

- (a) Dye, C. *Lancet* **2006**, 367, 938; (b) World Health Organization (WHO), *Fact Sheet No. 104: Tuberculosis*, **2007**.
- Davies, P. D. O.; Yew, W. W. *Expert Opin. Invest. Drugs* **2003**, 12, 1297.
- (a) Farmer, P.; Kim, J. Y. *Br. Med. J.* **1998**, 317, 671; (b) *Treatment of Tuberculosis: Guidelines for National Programmes*, 3rd ed.; World Health Organization, Geneva; 2004.
- (a) Marris, E. *Nature* **2006**, 443, 131; (b) Centers for Disease Control and Prevention (CDC), *Morbidity and Mortality Weekly Report*, **2006**, 55, 301.
- (a) Adams, J. M. *J. Mol. Biol.* **1968**, 33, 571; (b) Adams, J. M.; Capecchi, M. *Proc. Natl. Acad. Sci. U.S.A.* **1966**, 55, 147.
- (a) Chan, P. F.; O'Dwyer, K. M.; Palmer, L. M.; Ambrad, K. A.; Ingraham, K. A.; So, C.; Lonetto, M. A.; Biswas, S.; Rosenberg, M.; Holmes, D. J.; Zalacain, M. *J. Bacteriol.* **2003**, 185, 2051; (b) Mazel, D.; Pochet, S.; Marliere, P. *EMBO J.* **1994**, 13, 914; (c) Yuan, Z.; Trias, J.; White, R. J. *Drug Discov. Today* **2001**, 6, 954; (d) Clements, J. M.; Ayscough, A. P.; Keavey, K.; East, S. P. *Curr. Med. Chem. Anti-Infect. Agents* **2002**, 1, 239; (e) Leeds, J. A.; Dean, C. R. *Curr. Opin. Pharmacol.* **2006**, 6, 445.
- (a) Pei, D. *Emerg. Ther. Targets* **2001**, 5, 23; (b) Giglione, C.; Pierre, M.; Meinel, T. *Mol. Microbiol.* **2000**, 36, 1197.
- (a) Chen, D.; Yuan, Z. *Expert Opin. Invest. Drugs* **2005**, 14, 1107; (b) Johnson, K. W.; Lofland, D.; Moser, H. E. *Curr. Drug Targets Infect. Disord.* **2005**, 5, 39; (c) Ramanathan-Girish, S.; McColm, J.; Clements, J. M.; Taupin, P.; Barrowcliffe, S.; Hevizi, J.; Safrin, S.; Moore, C.; Patou, G.; Moser, H. *Antimicrob. Agents Chemother.* **2004**, 48, 4835.
- Teo, J. W. P.; Thayalan, P.; Beer, D.; Yap, A. S. L.; Nanjundappa, M.; Ngew, X.; Duraiswamy, J.; Liung, S.; Dartois, V.; Schreiber, M.; Hasan, S.; Cynamon, M.; Ryder, N. S.; Yang, X.; Weidmann, B.; Bracken, K.; Dick, T.; Mukherjee, K. *Antimicrob. Agents Chemother.* **2006**, 50, 3665.
- Pichota, A.; Duraiswamy, J.; Yin, Z.; Keller, T. H.; Schreiber, M. WO 2007077186 A1 20070712; *Chem. Abstr.* **2007**, 147, 166191.
- Patel, D. V.; Yuan, Z.; Jain, R. K.; Lewis, J. G.; Jacobs, J.; WO 2002102791 A1 20021227; *Chem. Abstr.* **2002**, 138, 55864.
- Balboni, G.; Salvadori, S.; Guerrini, R.; Negri, L.; Giannini, E.; Jinsmaa, Y.; Bryant, S. D.; Lazarus, L. H. *J. Med. Chem.* **2002**, 45, 5556.
- Almquist, R. G.; Chao, W. R.; Jennings-White, C. J. *Med. Chem.* **1985**, 28, 1067.

14. Pratt, L. M.; Beckett, R. P.; Davies, S. J.; Launchbury, S. B.; Miller, A.; Spavold, Z. M.; Todd, R. S.; Whittaker, M. *Bioorg. Med. Chem. Lett.* **2001**, *11*, 2585.
15. Jain, R.; Sundram, A.; Lopez, S.; Neckermann, G.; Wu, C.; Hackbarth, C.; Chen, D.; Wang, W.; Ryder, N. S.; Weidmann, B.; Patel, D.; Trias, J.; White, R.; Yuan, Z. *Bioorg. Med. Chem. Lett.* **2003**, *13*, 2373.
16. (a) Guilloteau, J. P.; Mathieu, M.; Giglione, C.; Blanc, V.; Dupuy, A.; Chevrier, M.; Gil, P.; Famechon, A.; Meinzel, T.; Mikol, V. *J. Mol. Biol.* **2002**, *320*, 951; (b) Kreusch, A.; Spraggon, G.; Lee, C. C.; Klock, H.; McMullan, D.; Ng, K.; Shin, T.; Vincent, J.; Warner, I.; Ericson, C.; Lesley, S. A. *J. Mol. Biol.* **2003**, *330*, 309; (c) Smith, K. J.; Petit, C. M.; Aubart, K.; Smyth, M.; McManus, E.; Jones, J.; Fosberry, A.; Lewis, C.; Lonetto, M.; Christensen, S. B. *Protein Sci.* **2003**, *12*, 349.
17. (a) Nikaido, H. *Cell Dev. Biol.* **2001**, *12*, 215; (b) Silva, P. E. A.; Bigi, F.; De La Paz Santangelo, M.; Romano, M. I.; Martin, C.; Cataldi, A.; Ainsa, J. A. *Antimicrob. Agents Chemother.* **2001**, *45*, 800; (c) Danilchanka, O.; Mailaender, C.; Niederweis, M. *Antimicrob. Agents Chemother.* **2008**, *52*, 2503.
18. Cynamon, M. H.; Alvarez-Freites, E.; Yeo, A. E. T. *J. Antimicrob. Chemother.* **2004**, *53*, 403.
19. A lower culture inoculum was used in the TB assay compared to the BCG assay (10^5 vs 10^6 CFU/ml) causing the systematically lower MICs.
20. The details of structure refinement are summarized in the supplementary material. Coordinates of the final structure have been deposited in the RCSB Protein Data Bank under the accession number 3E3U.
21. Saxena, R.; Chakraborti, P. K. *J. Bacteriology* **2005**, *187*, 8216.
22. Saxena, R.; Chakraborti, P. K. *Biochem. Biophys. Res. Commun.* **2005**, *332*, 418.